Structure and Dynamics of Jupiter's Duskside Magnetosphere

The goal of the proposed work is to use Juno extended mission data to characterize the structure and dynamics of Jupiter's duskside magnetosphere, a local time region that has been relatively poorly studied compared to the dawn sector. We will determine the properties of Jupiter's duskside lobe field and the latitudinal dependence of the field bendback angle and its implications for the aurora. We will also compare Juno data to model predictions of plasma heating in the afternoon sector that explains plasma sheet thickening near dusk. Our results will help establish the causes of local time asymmetries in Jupiter's magnetosphere.

Jupiter's magnetosphere, illustrated in Figure 1, is the largest in the solar system on both absolute and relative (to the planetary radius) terms, with a typical magnetopause standoff distance of ~60-90 R_J (Jovian radii, 1 R_J = 71492 km) depending on the solar wind dynamic pressure. The primary source of plasma in Jupiter's magnetosphere is the volcanically active moon Io, which contributes ~500–1,000 kg/s of plasma in the form of sulfur and oxygen ions (e.g. Thomas et al., 2004). The magnetosphere's large size is due in part to the strong planetary magnetic field and the presence of hot plasma, which is largely confined to the magnetodisk or plasma sheet near the magnetic equator. In the magnetotail the regions above the plasma sheet, called the lobes, feature low density plasma and highly radially stretched magnetic field. Jupiter's internal dipole field is tilted by ~10º with respect to its rotation axis meaning that the plasma sheet, which is located near the magnetic equator, passes over the jovigraphic equator twice per Jovian rotation.

Jupiter's magnetosphere displays strong local time asymmetries in quantities such as the magnetic field , plasma sheet thickness, and flows derived from energetic particles (e.g. Arridge et al., 2015; Palmaerts et al., 2017). Ultimately these local time asymmetries arise because of the nature of the solar wind flowing past an obstacle, in this case Jupiter's rapidly-rotating magnetosphere. For example, the solar wind confines Jupiter's magnetosphere on the day side through pressure balance between the magnetospheric magnetic and thermal pressures and the solar wind dynamic or ram pressure, while on the night side the solar wind stretches the magnetic field in the anti-sunward direction, forming the magnetotail. In Jupiter's magnetosphere, centrifugal stresses are significant due to the large spatial scales and rapid planetary rotation period

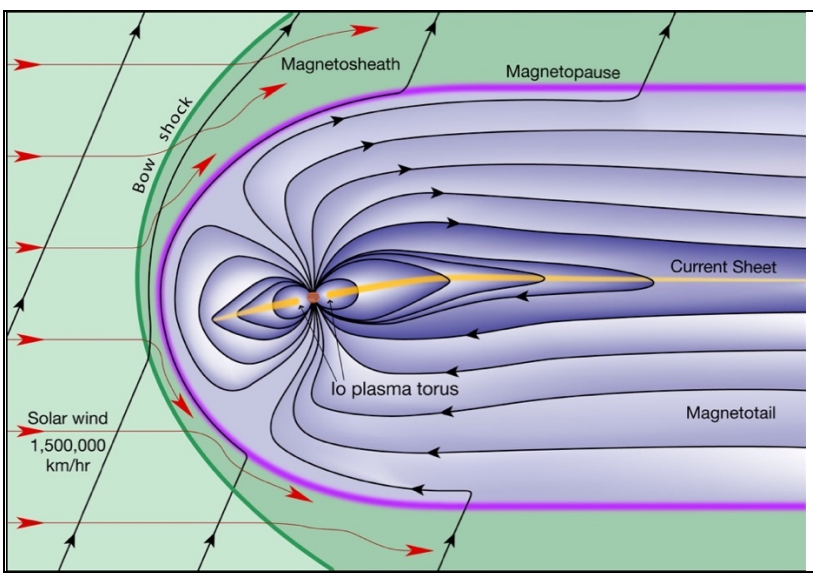

Figure 1. Illustration of Jupiter's magnetosphere, shown here in a meridian plane, including the Io plasma torus and current sheet. The overall shape of the magnetosphere (rounded on the dayside, extended magnetotail on the nightside) is one example of a solar wind-induced local time asymmetry. Arrows indicate the magnetic field direction. Courtesy: Fran Bagenal and Steve Bartlett, LASP MOP website.

(~10 h), such that both the solar wind *and* rotational dynamics contribute to Jupiter's magnetospheric local time asymmetries.

When considering local time asymmetries in Jupiter's magnetosphere it is important to note that, in general, the structure and dynamics of Jupiter's middle and outer magnetosphere have been significantly better studied at midnight to dawn local times than at dusk to midnight local times. The pre-Juno spacecraft coverage of Jupiter's middle and outer magnetosphere is significantly better at midnight-dawn local times than at dusk-midnight local times, as shown in **Figure 2**. **(**The Galileo orbital tracks, drawn in purple in the top panel of **Figure 2**, are somewhat misleading because much of the duskside Galileo data has a low time resolution –often 1800 s per vector for duskside magnetometer data, compared to a typical resolution of 24 s per vector on the dawn side.) There is significantly more data available from dawn local times than from dusk local times, particularly beyond ~60 R_J.

Despite the disparate local time coverage, Galileo data have clearly demonstrated through that the plasma sheet is thicker near dusk (half thickness > 6 R_J) than it is at dawn (2-3 R_J half thickness) (Khurana, 1992; Khurana and Schwarzl, 2005), and azimuthal flows inferred from the particle anisotropies measured by the Energetic Particle Detector (EPD) are stronger at dawn than at dusk (Krupp et al., 2001). For example, in **Figure 3** the thicker plasma sheet near dusk than at

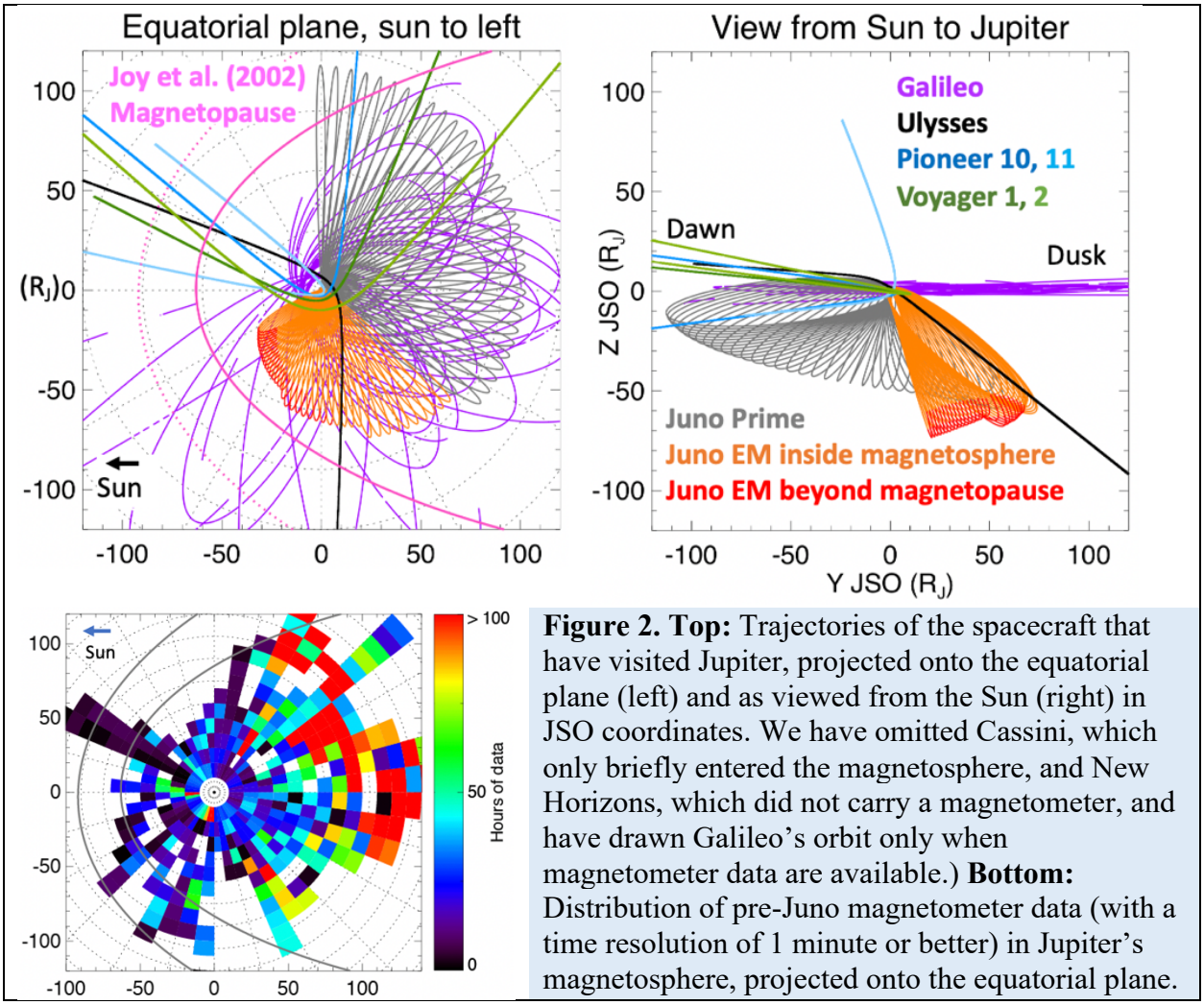

Figure 2. Top: Trajectories of the spacecraft that have visited Jupiter, projected onto the equatorial plane (left) and as viewed from the Sun (right) in JSO coordinates. We have omitted Cassini, which only briefly entered the magnetosphere, and New Horizons, which did not carry a magnetometer, and have drawn Galileo's orbit only when magnetometer data are available.) **Bottom:** Distribution of pre-Juno magnetometer data (with a time resolution of 1 minute or better) in Jupiter's magnetosphere, projected onto the equatorial plane.

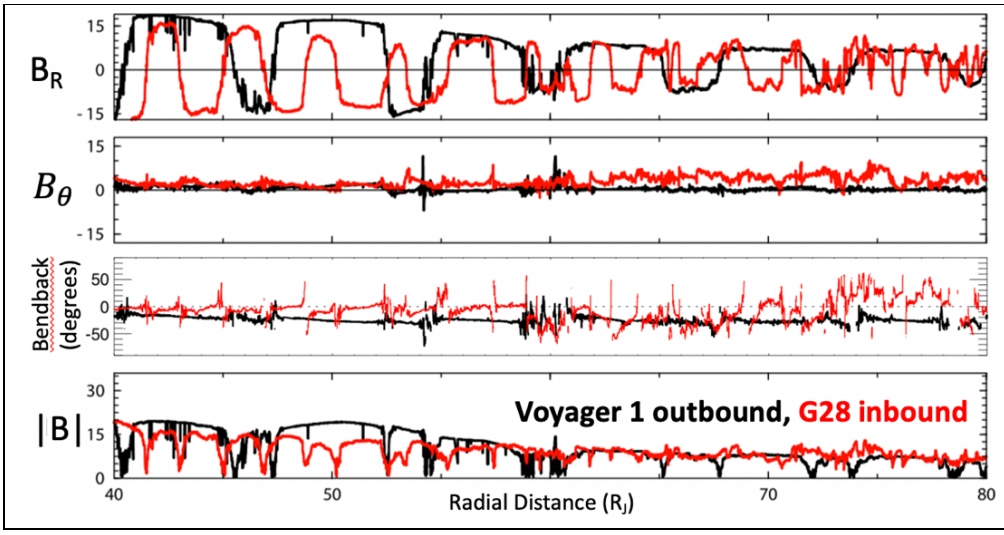

Figure 3. Magnetic field components, field bendback, and |B| as a function of radial distance for **Voyager 1 near dawn** and **Galileo orbit G28 near dusk**. Modified from Vogt et al. (2014b).

dawn can be seen by the increased B_θ , the meridional component of the magnetic field, and absence of the ~10 hour square wave signature in B_R, the radial component of the magnetic field. Because of Jupiter's ~10º dipole tilt the plasma sheet will pass over a spacecraft located at the Jovigraphic equator every ~5 hours, resulting a square wave signature in B_R and B_φ. The Galileo duskside radial field B_R in **Figure 3** is disordered compared to the flat-topped square wave in the Voyager 1 dawnside B_R field, indicating that Galileo did not exist the plasma sheet.

Local time asymmetries in some data sets or magnetospheric properties have not been well-characterized or feature inconsistencies. One example is the magnetic field "bendback", or the field's leading or lagging configuration out of a meridian plane. The equatorial Galileo data in **Figure 4** show that the field bendback changes with radial distance, typically becoming larger in magnitude in the middle and outer magnetosphere. Except at large radial distances near the magnetopause, the equatorial duskside Galileo bendback in **Figure 3** show a negative bendback angle like the dawn Voyager data. In general duskside Galileo data show a typical lagging configuration (blue) at radial distances ~30-60 R_J **(Figure 4, left)** but the high-latitude Ulysses magnetic field data show consistent leading configuration (red) at and beyond those distances **(Figure 4, middle)**. Kivelson et al. (2002) noted that the difference "could be attributed to temporal effects" but proposed instead that it results from a latitude-dependent field shear. However, some of the evidence they presented in favor of this argument came from large radial distances, near the magnetopause, where a leading field configuration would be expected not from a field shear but from the interaction with the magnetopause boundary as the solar wind pulls the field tailward. Additional high latitude dusk data are needed to characterize the field shear and its expected impact on the duskside aurora.

Finally, some questions about the magnetospheric variability with local time remain unanswered because all data have not been thoroughly analyzed. For example, using the Galileo magnetometer data that were available at the time (through May 2000), Kivelson and Khurana (2002) examined the spatial distribution of tail lobe magnetic pressure (see **Figure 5**) and Khurana (2001) calculated the distribution of currents in the equatorial plane, including the field-aligned currents that influence the aurora. However, Galileo collected magnetometer data through the end of 2002, so the analysis in those two studies omitted critical data from 6 subsequent Galileo orbits in the noon-dusk local time sector. Expanding that analysis using the full Galileo dataset and measurements from Juno's prime and extended mission will provide a more complete picture of the local time dependence of the magnetic field structure in Jupiter's magnetosphere. For example,

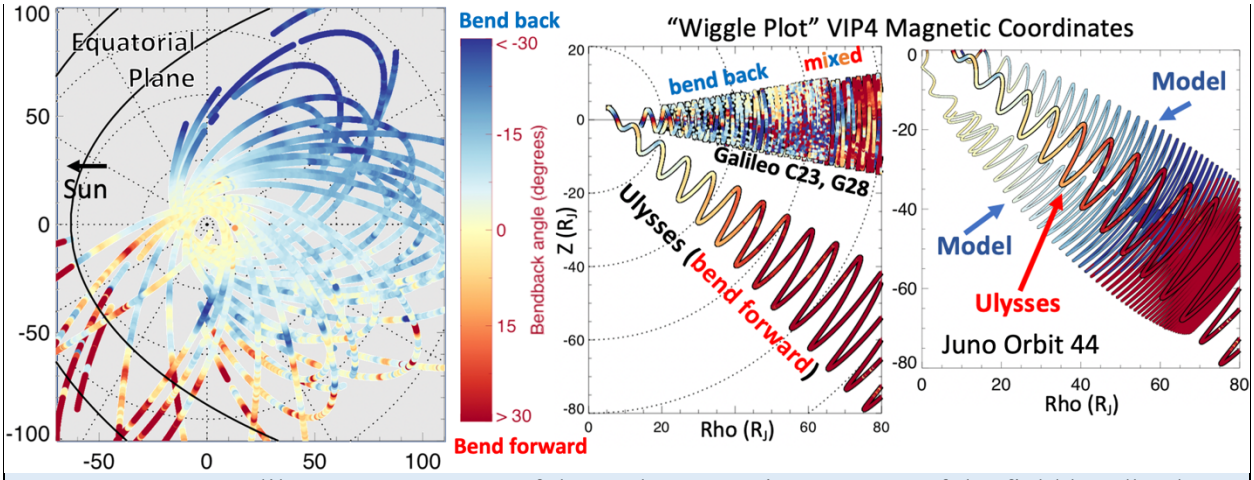

Figure 4. (Left) Galileo measurements of the 10-hour running average of the field bendback angle (blue = bent back, red = bent forward) in the equatorial plane. **(Middle)** "Wiggle plot" of Galileo orbits C23 and G28 and Ulysses orbital trajectory in cylindrical magnetic coordinates, with color indicating the measured bendback angle. **(Right)** Wiggle plot of the trajectory for Juno orbit 44 (color indicating the VIP4+CAN2020 model bendback) and Ulysses.

Kivelson and Khurana (2002) reported large error bars for the duskside lobe pressures beyond ~40 R_J (**Figure 5, right**), and additional data would help ascertain whether this results from the limited data coverage there or whether the lobe field is more variable near dusk. We note also that Lorch et al. (2020) recently expanded Khurana (2001)'s analysis, including all Galileo data and the available Juno data from the dawn local time sector, and found new evidence for current closure in the dusk-noon magnetosphere.

Ultimately, fully characterizing the nature of local time asymmetries in Jupiter's magnetic field and plasma properties provides important observational constraints for conceptual models of plasma and energy circulation in Jupiter's magnetosphere. As Arridge et al. wrote in a 2015 review paper, "(a) key physical question that remains to be solved is whether local time asymmetries require solar wind-driven convection (via viscous interaction or reconnection) or if we can explain these asymmetries in terms of internal/rotational processes operating in an asymmetrical cavity formed by the normal stress of the solar wind." For example, the conceptual model from Kivelson and Southwood (2005) proposes the influence of rotational stresses on plasma heating as one explanation for the plasma sheet thickening that occurs between noon and dusk local times. They note that flux tubes expand non-adiabatically as they rotate through the noon to dusk local time sector because of Jupiter's rapid rotation period and that the centrifugal force adds energy during this expansion but only in the direction parallel to the magnetic field. This creates a pressure anisotropy that leads to ballooning through a "centrifugal instability", and the plasma sheet thickens (increased scale height) due to the increased thermal energy. A competing explanation for the plasma sheet thickening near dusk is that corotational flow on the dusk side is opposed by sunward return flow from tail reconnection at a distant neutral line (Khurana et al., 2004). The increased plasma sheet thickness near dusk can be explained if convection of the solar wind-driven Dungey cycle (Dungey, 1961) in Jupiter's magnetotail is restricted to a single cell on the dawn side, which would lead to an asymmetric distribution of open flux across the magnetotail (Cowley et al., 2003). This explanation accounts for the slower EPD azimuthal flows at dusk, though Galileo tail reconnection observations have not found evidence of a duskside x-line (Woch et al., 2002; Vogt et al., 2010). Additionally, Delamere and Bagenal (2010) describe a conceptual model of the implications of a viscous interaction with the solar wind

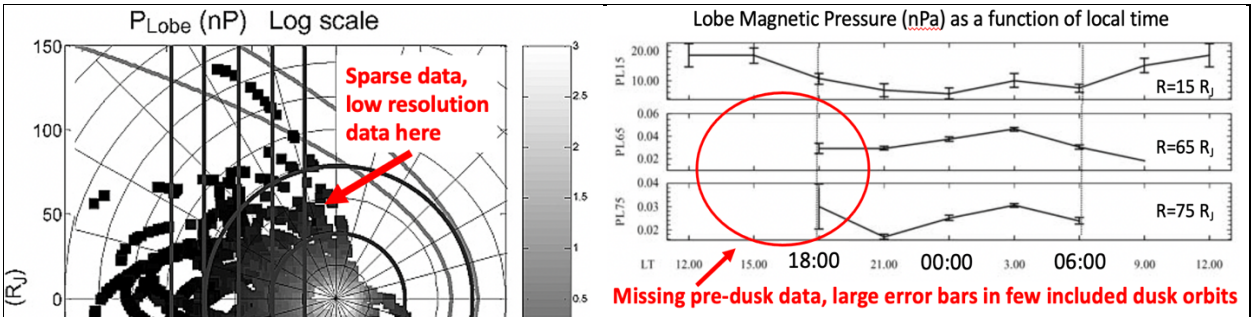

Figure 5. Modified from Kivelson and Khurana (2002). **(Left)** Distribution of the lobe magnetic pressure in the equatorial plane. The duskside data coverage is limited compared to dawn, and looks more complete than it is because of the large size of the plotted symbols. **(Right)** Lobe magnetic pressure as a function of local time in three radial distance bins.

at the magnetopause, including local time asymmetries in the magnetic field and plasma properties. Some aspects of the various conceptual models are mutually exclusive, so we look to Juno EM data to provide additional observational constraints.

Characterizing the structure and dynamics of the duskside magnetosphere is an important first step toward understanding what processes contribute to Jupiter's local time asymmetries and, ultimately, understanding how mass and energy flow through the Jovian magnetosphere. Unfortunately, as discussed above, the existing (pre-Juno) magnetic field and plasma measurements provide an incomplete picture of the dusk magnetospheric structure. and variability (both spatial and temporal). Juno's extended mission (EM) will provide the first measurements since the brief Ulysses flyby of the duskside magnetosphere at high latitudes. The off-equatorial observations are particularly valuable for understanding the structure of the dusk plasma sheet and tail lobes, since many near-equatorial duskside Galileo orbits never or rarely exited the plasma sheet. The additional spatial and temporal coverage provided by Juno EM data, particularly through comparison to the Ulysses high latitude flyby data, will help characterize the effects of internal magnetospheric activity and changes in the upstream solar wind.

The goal of our proposed work is to improve our understanding of the structure and dynamics of Jupiter's duskside magnetosphere through analysis of Juno EM data. Our work will address the following questions:

1) **What are the properties of Jupiter's duskside lobe field?**
2) **What is the structure and variability of the magnetic field bendback in Jupiter's duskside magnetosphere and how does it influence the aurora?**
3) **Why is Jupiter's plasma sheet thickest near dusk?**

Our work will involve analysis of Juno *in situ* magnetic field and plasma data, as well as UVS auroral images. We will analyze periodic fluctuations in the radial and azimuthal components of the magnetic field data to identify trends in how the plasma sheet and lobe properties vary with radial distance and local time. We will also use Juno magnetic field data to determine the latitudinal dependence of the magnetic field bendback and its variability, then calculate the expected field-aligned currents (FACs) and their variability. We will compare our findings to auroral images. Finally, we will compare Juno data, particularly the plasma energy and pitch angle distributions

from the JEDI and JADE instruments, to model predictions to determine how plasma is energized in the afternoon local time sector, testing the conceptual model of Kivelson and Southwood (2005).

In addition to the data analysis work described above, we will also run a solar wind propagation model to predict the solar wind conditions upstream of Jupiter during the Juno EM. Knowledge of the upstream solar wind conditions provides a useful constraint on the possible driver(s) of magnetospheric variability and the process(es) that produce magnetospheric dawn-dusk asymmetries. Roughly the latter half of Juno's EM orbits will cross the predicted location of the Joy et al. (2002) compressed magnetopause, with the spacecraft possibly being located in the magnetosheath for ~several days near apoapsis if the solar wind dynamic pressure is high (red lines in **Figure 1**). However, if Juno does not cross the magnetopause we cannot deduce the spacecraft's proximity to the magnetopause without additional information about the predicted solar wind conditions upstream of Jupiter, particularly since the magnetopause location is so unconstrained at high latitudes. For example, if Juno does not observe any magnetopause crossings during its EM that could mean that the solar wind dynamic pressure was consistently low *or* that the compressed magnetopause is located farther away than the Joy model predicts. The availability of predicted upstream solar wind conditions from our model will help distinguish between those two scenarios and will contribute to other Juno science team activities as we discuss below.

2. Data to be used in this study

Juno is carrying a suite of instruments that measure the magnetic field and plasma properties in Jupiter's magnetosphere. During Juno's extended mission (EM) the spacecraft will pass through the afternoon to post-dusk local time sectors, in an inclined orbit with apoapsis ranging from ~80 to ~100 R_J (see **Figure 2**). In our work we will use Juno EM data from:

- **MAG** (Magnetometer; Connerney et al., 2017) – Vector fluxgate magnetometer measuring the magnetic field components; we will use data with a time resolution of 1 second per vector
- **JEDI** (Juno Energetic particle Detector Instrument; Mauk et al., 2017) – Measures energy and pitch angle distributions for electrons from 40 to 500 keV and energy, pitch angle, and ion composition distributions for ions at ~20-50 keV to more than 1 MeV. Time resolution as high as 0.5 seconds in the auroral region.
- **JADE** (Jovian Auroral Distributions Experiment; McComas et al., 2017) – Provides energy spectra and pitch angle distributions for electrons at 0.1-100 keV and ions 5 eV - 50 keV, also measures ion composition from 1 to 50 amu. Time resolution ranges from 30 seconds to 10 minutes in low rate science mode depending on bandwidth.
- **Waves** (Juno WAVES Investigation; Kurth et al., 2017) – Provides electric spectra at frequencies 50 Hz to 40 MHz and magnetic spectra at frequencies 50 Hz to 20 kHz, with a time resolution of 30 seconds per spectra (in apoapsis mode).
- **UVS** (Ultraviolet Spectrograph; Gladstone et al., 2014) – a photon-counting imaging spectrograph with a spectral range of 68-210 nm. The Juno-UVS slit is oriented perpendicular to the spin plane of Juno and as such scans across the sky every spin. Complete maps of Jupiter's auroral regions are produced by stepping the scan mirror between consecutive spins and then stitching scan maps together.

We will compare Juno duskside EM data to data from the Ulysses flyby. Where appropriate, we will extend our analysis to include data from the Galileo magnetometer (Kivelson et al., 1992), Energetic Particle Detector (EPD) (Williams et al., 1992), and plasma science instrument (PLS) (Frank et al., 1992), which are all available from the Planetary Data System (PDS), https://pds-

ppi.igpp.ucla.edu/mission/Galileo. The Galileo data can complement the Juno spatial coverage, and, as mentioned above, some duskside Galileo orbits have not yet been thoroughly analyzed. We will also complement the Juno UVS auroral images with past and upcoming images from the Hubble Space Telescope (e.g. Grodent et al., 2018).

Finally, we will run a 3-D MHD solar wind propagation model to predict the solar wind conditions upstream of Jupiter during Juno's EM, which can be helpful for determining whether any observed magnetospheric activity was solar wind or internally driven. Though *not required to successfully achieve our science objectives*, we anticipate being able to also compare the observed magnetospheric activity to changes in the Io plasma torus that would indicate internal driving. For example, Juno's EM will "(i)nvestigate the spatial and temporal variability of the Io and Europa plasma tori to address the transport of mass and energy through Jupiter's inner magnetosphere" (Juno PS Proposal Information Package, or PIP). Additionally, Juno radio occultations can make measurements of the Io plasma torus electron density once per Juno orbit (e.g. Phipps et al., 2018, 2019). Finally, ground-based Io observations are ongoing, for example "IoIO", the Io Input/Output facility, is supported through at least 2023 to measure the sodium nebula (Na 5893Å) and S+ torus ([SII] 6731 Å) brightness, which can yield torus densities (Morgenthaler et al., 2019).

3. Summary of proposed research

Our work will be divided into 4 tasks, each addressing at least one motivating science question:

Task	Description	Science Question(s)
A	Identify lobe field intervals & calculate 2-D fits to lobe magnetic pressure	1,3
B	Characterize the duskside magnetic field bendback & calculate FACs	2
C	Characterize how duskside plasma energy & pitch angle distributions evolve with local times and compare to model predictions	3
D	Run SWMF-OH solar wind propagation model	1,2,3

3.1 Task A: Identify lobe field intervals and calculate 2-D fits to the lobe magnetic pressure

We will use Juno magnetometer data to identify regions of lobe field, calculate the magnetic pressure in the lobes and plasma sheet, and characterize the spatial and temporal variability of the duskside lobe field. While some previous works (Khurana, 2001; Kivelson and Khurana, 2002) have identified the lobe field via visual inspection, selecting for regions where B_R and B_φ reach plateaus, we will identify lobe field regions with an automated routine. For example, Lorch et al. (2020) successfully applied an algorithm to Galileo and dawn side Juno orbits by selecting for plateaus in B_R, which they defined as regions with a deviation of less than ±7.5% for 30 minutes. Based on our inspection of the high-latitude Ulysses data we expect a similar approach will be successful in identifying the lobe field regions in the Juno EM data. If necessary, we will adjust the algorithm to identify, for example, regions where B_R and B_φ vary slowly with distance from the magnetic equator rather than identifying regions where B_R and B_φ vary slowly in time. The focus of our work will be on Juno magnetometer data but we will also incorporate JADE and JEDI data in our analysis to help identify the location and particle/plasma properties of the low-density lobe regions, with particular interest in the ion composition which may yield information about whether the lobe field lines are open or closed.

After identifying regions of lobe field we will calculate the magnetic pressure in the lobes ($p_{lobe} = |B_{lobe}|/2\mu_0$, where μ_0 is the permeability of free space) and compare it to the expected

magnetic pressure at the center of the plasma sheet. Though Juno is unlikely to pass through the center of the plasma sheet, the magnetic pressure there can be estimated from B_Z, the north-south component (in magnetic coordinates) of the magnetic field, in the lobe, following Kivelson and Khurana (2002). Their approach is based on the divergence-free nature of the field ($\nabla \cdot \boldsymbol{B} = 0$) and the assumption that "the scale length of the magnetic field variation in z is small compared with the scale lengths of variations in radius and azimuth" such that $\partial B_z/\partial z \approx 0$. The magnetic pressure in the plasma sheet is therefore $p_{B,PS} = |B_{z,PS}|/2\mu_0$ and we can then estimate the thermal pressure in the plasma sheet, $p_{T,PS}$, via pressure balance argument: $p_{lobe} = p_{B,PS} + p_{T,PS}$.

For p_{lobe}, $p_{B,PS}$, and $p_{T,PS}$ we will then create plots like **Figure 5**, which is modified from Kivelson and Khurana (2002)'s Figure 2, and develop 2-D (radial distance and local time) fits. We have successfully created these types of 2-D magnetic field fits before (Vogt et al., 2011) but if we encounter difficulties in the 2-D fitting proposed here (and also in Task B) we can perform simple radial fits separately for different local time sectors (dusk, pre-midnight, etc.). We will also look for temporal variability in the lobe field and search for evidence of links to, for example, increases in the solar wind dynamic pressure. Our approach will be guided by our experience identifying transient increases in $|B|$ measured by Galileo and using a statistical analysis to establish a link to the predicted upstream solar wind dynamic pressure (Vogt et al., 2019).

Finally, we note that our work will be focused on the Juno EM data but we will include Galileo duskside orbits, especially those that were not included in the Kivelson and Khurana (2002) study. The Galileo orbits alone are insufficient for our study because of their low time resolution and near-equatorial orbit, meaning that the spacecraft often never fully exited the duskside plasma sheet. We will also apply our lobe identification algorithm to earlier Juno orbits at midnight to dawn local times to determine how properties of the lobe field vary in local time. We plan to analyze all Juno orbits since we will be using an algorithm that can be applied to additional orbits with minimal additional effort. However, if we encounter any difficulties applying the algorithm to dawn sector orbits we can identify the lobe field using visual inspection in just a few representative Juno orbits from midnight-dawn. We will compare our findings to the results of Kivelson and Khurana (2002). Finally, we will examine how the location of the identified lobe field intervals (specifically, the height above the magnetic equator) compares for dawn and dusk orbits, from which we can infer information about the plasma sheet thickness and the distribution of open flux across the tail.

<u>Expected results and their significance:</u> We will establish how the magnetic pressure varies with radial distance and local times in Jupiter's magnetospheric lobes. Our analysis will expand on previous work (Kivelson and Khurana, 2002) by filling in gaps at local times ~15:00-21:00 and increasing the coverage at ~18:00-21:00. We will create 2-D fits and plots like **Figure 5** for the lobe magnetic pressure and the plasma sheet magnetic and thermal pressures. The derived local time evolution of the plasma sheet thermal pressure will be used in the data-model comparison work described in section 3.3 below (Task C). Our results will establish the nature of local time asymmetries in the lobe properties and therefore provide information about the plasma sheet thickness and distribution of open flux across the magnetotail, which informs our understanding of global magnetospheric dynamics.

3.2 Task B: Characterize the duskside field bendback & calculate FACs

We will use Juno magnetometer data to calculate α, the magnetic field bendback angle ($\alpha = \tan^{-1}\frac{B_\varphi}{B_R}$) along the spacecraft orbit. The bendback angle is defined such that it is positive if

the field is swept forward (leading corotation) and negative if the field is swept back (lagging corotation). When B_R is small, α changes rapidly with small changes in B_R, so we will only calculate α when $|B_R| > 3$ nT, a condition which is only not met very close to the center of the plasma sheet. We will also calculate the 10-hour running average of the bendback angle and work with this quantity where appropriate to remove brief temporal changes and make it easier to study spatial changes with radial distance, local time, distance from the center of the plasma sheet, and distance to the magnetopause. Even for orbits for which a magnetopause crossing is not observed or expected, we can infer whether the magnetopause is in a compressed or expanded state using the predicted solar wind dynamic pressure we will obtain from Task D.

Our work will focus on Juno EM orbits in the pre-midnight local time sector. We will determine whether α is typically positive, indicating a leading field configuration, at high latitudes as was observed by Ulysses and hinted at with Galileo data. We will take several steps to characterize the nature of the field bendback in the dusk local time sector (roughly 15:00-21:00 LT), including compiling statistics on α and developing a functional form to describe its spatial variability. If Juno data confirm that the field configuration is typically sheared, with a bent back field configuration ($\alpha < 0$) near the equator and a bent forward field configuration ($\alpha > 0$) at high latitudes, we will characterize the properties of the field shear, including compiling statistics on the magnitude and spatial extent of the field shear (at what radial distances is it typically observed and what heights with respect to the magnetic equator) and calculating the associated FACs. If the nature of the field shear is found to be highly variable then we will perform a few detailed case studies calculating the FACs from Ampere's Law. Otherwise we will calculate the spatial distribution of the typical field-aligned current following the approach of Khurana and Schwarzl (2005) and Lorch et al. (2020). We will compare our predicted FACs and their mapped auroral locations (e.g. Vogt et al., 2011, 2015) to HST and Juno UVS images, with particular interest in whether we can explain observations of multiple dusk arcs **(Figure 6)**.

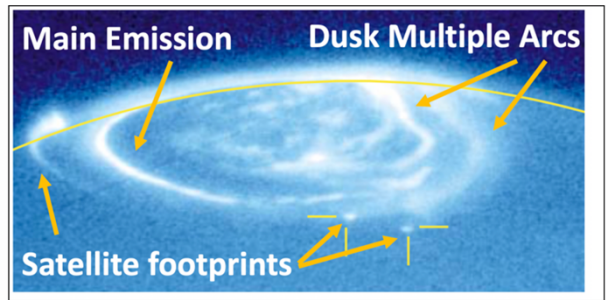

Figure 6. (Left) Illustration of the FAC system in Jupiter's magnetosphere, from Kivelson et al. (2002). **(Right)** HST image of Jupiter's UV aurora (Clarke et al., 2002).

We will compare bendback measurements from successive orbits to determine how it varies in time and will examine the predicted upstream solar wind conditions obtained from Task D to determine whether the variability is linked to changes in the solar wind. For example, one may expect that the field would become increasingly bent forward (α would become more positive) in response to an increase in the solar wind dynamic pressure for two reasons. First, as the magnetosphere is compressed, plasma from the outer magnetosphere moves radially inward and its azimuthal velocity should increase as it moves inward to conserve angular momentum. Since the field is frozen into the flow the field should become increasingly bent forward. Second, an increase in the solar wind dynamic pressure would also increase the corotation lead of the field as it increases the solar wind's tailward flow and enhances the processes that transfer mass and momentum across the magnetopause boundary.

Finally, as time allows, we will repeat much of the above statistical analysis of the field bendback on data from earlier Juno orbits at midnight to dawn local times to determine the properties of the bendback angle in the high-latitude (relative to Galileo, but lower latitude than at

dusk) dawn Juno orbits. As in Task A, we will plan to analyze all Juno orbits to fully characterize the local time dependence, but will scale back our plans and consider just a few orbits, each representing a different local time sector, if necessary.

Expected results and their significance: We will characterize the latitudinal dependence of the magnetic field bendback in the dusk local time sector and definitively resolve the inconsistency between Ulysses flyby observations of a bent forward field at high latitudes and Galileo observations of a bend back field near the equatorial plane. Our results will provide information about the expected FACs and dawn-dusk asymmetries in Jupiter's magnetosphere-ionosphere coupling. Additionally, our results in this local time region will provide a useful constraint to global magnetic field models (e.g. Khurana, 1997 and unpublished "kk2009" model; Connerney et al., 2020), which do not presently reproduce the Ulysses observations of bend forward at high latitudes. For example, the VIP4 + CAN2020 (Connerney et al., 1998, 2020) modeled bendback angle along Juno orbit 44, is bent back in regions where Ulysses measured a consistent bend forward (see **Figure 4**).

3.3 Task C: Characterize how duskside plasma energy & pitch angle distributions evolve with local times and compare to model predictions

Juno's EM orbital trajectory provides an excellent opportunity to examine how magnetospheric properties evolve as field lines rotate from the late afternoon through dusk into the pre-midnight local time sector, expanding outward due to with the decrease pressure from the increasingly-distance magnetopause boundary. In this task we will use Juno JADE and JEDI data to test the Kivelson and Southwood (2005) conceptual model of rotationally-driven dynamics, specifically the predictions that the plasma sheet thickening near dusk is produced when non-adiabatic field line stretching creates a pressure anisotropy that leads to a "centrifugal instability" and plasma sheet ballooning and thickening.

A key point in the Kivelson and Southwood (2005) argument is that the flux tube expansion occurs non-adiabatically because particle bounce times are long compared to the ~few hours it takes for field lines to rotate from the afternoon to evening local time sectors. The effects of adiabatic expansion in a rotating system can be determined through calculation of an energy constant that accounts for motion along the centrifugal potential as well as conservation of the first

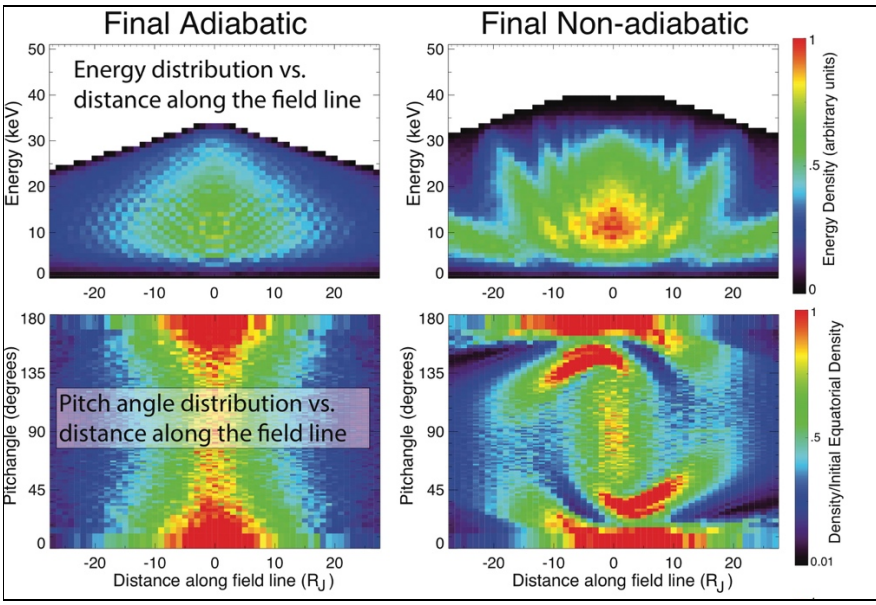

Figure 7. Modeled energy and pitch angle distributions along a sample field line after adiabatic (**left**) and non-adiabatic (**right**) stretching similar to the flux tube expansion between noon and dusk. Non-adiabatic stretching leads to larger densities at high latitude, increased energy, and a different pitch angle distribution. Modified from Vogt et al. (2014b).

adiabatic invariant μ (Northrup and Birmingham, 1982). However, for non-adiabatic expansion the change in a particle's energy or pitch angle cannot be determined analytically. Therefore, Vogt et al. (2014b) used a large-scale kinetic simulation to create a "toy model" that followed particles of 20 proton mass on an expanding flux tube in a system designed to mimic the properties of the magnetic field as it rotates from noon through dusk. Their results showed that the non-adiabatic nature of the field stretching led to larger densities at high latitude, increased energy, a more field-aligned pitch angle distribution, and an increased off-equatorial pressure anisotropy compared to the adiabatic case (**Figure 7**). They concluded that the model results were consistent with processes that would cause the plasma sheet to thicken. They noted, however, that the modeled anisotropies were likely an overestimate since their model did not include effects of pitch angle scattering.

We propose to use JADE and JEDI ion data to examine how the pitch angle distribution, energy distribution, and densities (or energy fluxes if moments are not available) evolve with local time over the mid-afternoon to post-dusk region. We will discard data from intervals of high solar wind dynamic pressure as predicted by the solar wind MHD modeling described in Task D to ensure our analysis focuses on the effects of the steady-state flux tube expansion that occurs as field lines rotate through this local time region and not on the effects of a solar wind-induced compression/expansion. We anticipate that our data-model comparison will be largely qualitative in nature, for example reporting or whether, and at what energies and locations, the model and data predict increasingly field-aligned pitch angles with increasing local time. Additionally, though Juno will not directly measure the duskside thermal pressure in the plasma sheet due to its highly inclined orbit, we will have estimated that quantity from Task A and can compare its local time evolution to the model predictions.

Vogt et al. (2014b) assumed an initially isotropic pitch angle distribution at noon, with initial Maxwellian and Kappa energy distributions with temperatures of ~2-10 keV, but changing the initial conditions is simply a matter of re-normalizing the weight given to each particle in the initial distribution functions. PI Vogt still has copies of all original data files from the simulation. Therefore, if necessary, we can change the "initial" conditions of the Vogt et al. (2014b) simulation to more closely match the Juno JADE and JEDI data at a reference local time other than noon. We can then re-normalize the particles according to the new the distribution function in the model output for every simulation time step (later local times) – all without having to create any additional model runs. This is particularly relevant since the earliest local time that will be sampled by Juno's EM orbits is ~13:00, at the end of the mission. Additionally, the modeled flux tube expansion should proceed in a similar manner for local times at ~1-2 hours pre- and post-dusk so the model output could be tweaked slightly, again without needing to re-run the LSK model, to expand our analysis to later local times. This will allow us to begin our data-model comparison at later local times while waiting for Juno's orbit to pass into the early afternoon local time sector.

<u>Expected results and their significance:</u> We will compare JADE and JEDI measured pitch angle and energy distributions to model results that tracked particle motion on non-adiabatically expanding flux tube in a system designed to mimic the properties of the field in Jupiter's noon-to-dusk magnetosphere. If we find good data-model qualitative agreement then we will conclude that the likely explanation for the thickening of the plasma sheet near dusk is a "centrifugal instability" caused by pressure anisotropies that arise due to the effects of non-adiabatic flux tube expansion in the afternoon sector of a rapidly-rotating magnetosphere. However, if we do not find good agreement one possible explanation could be the absence of pitch angle scattering in the LSK model, and we can test this by examining Juno Waves data.

3.4 Task D: Run SWMF-OH solar wind propagation model

Measurements of the solar wind conditions upstream of Jupiter are typically not available concurrently with *in situ* magnetospheric measurements, and this continues to be the case with Juno. Therefore, we must rely on models that propagate solar wind data measured at the Earth's orbit at 1 AU out to Jupiter's orbit at 5.2 AU. These models include a 1-D MHD model developed by Tao et al. (2005) that propagates OMNIWeb solar wind data from 1 AU out to the orbits of Jupiter and Saturn (model outputs are the solar wind density, the radial component of the solar wind velocity, the solar wind speed, and one component of the IMF) and the 1-D MHD Michigan Solar Wind Model (Zieger and Hansen, 2008; Zieger et al., 2009), known as mSWiM.

It is important to recognize that solar wind propagation models have limitations and are subject to timing errors, particularly when the Earth-Sun-Jupiter angle is large, that can be as long as a few tens of hours. Despite their limitations, solar wind propagation models have been widely adopted to predict the solar wind conditions upstream of Jupiter and Saturn: the paper describing the Tao model has nearly 100 citations and the paper describing the mSWiM model has over 100 citations according to Google Scholar as of August 2021.

In this task we will run a 2-D multi-fluid MHD solar wind propagation model, called SWMF-OH, to predict the solar wind conditions upstream of Jupiter during the Juno extended mission (June 2021 – September 2025). A significant advantage of the SWMF-OH model over the Tao model or mSWiM is that it can predict all three components of the interplanetary magnetic field. 1-D MHD models cannot propagate B_R because of the divergence-free nature of the magnetic field (see discussion in Zieger and Hansen, 2008). Predicting the IMF is crucial for fully understanding the interaction between the solar wind and Jupiter's magnetosphere, for example in determining whether the IMF orientation was favorable for dayside reconnection. Additionally, SWMF-OH does a good job of predicting intervals of increased solar wind P_{Dyn} from corotating interaction regions even when the Earth-Sun-Jupiter angle is large.

SWMF-OH was adapted by Collaborator Bertalan Zieger from the outer heliosphere (OH) component of the Space Weather Modeling Framework (SWMF) (Tóth et al., 2012), which is a 3-D global multi-fluid MHD model of the outer heliosphere with one ion fluid and four neutral populations (Opher et al., 2006; 2009). It provides time-dependent 2-D multi-fluid MHD simulations of solar wind propagation from a heliocentric distance of 1 AU up to 50 AU. Model inputs are hourly OMNI data of the measured solar wind density, velocity, magnetic field, and

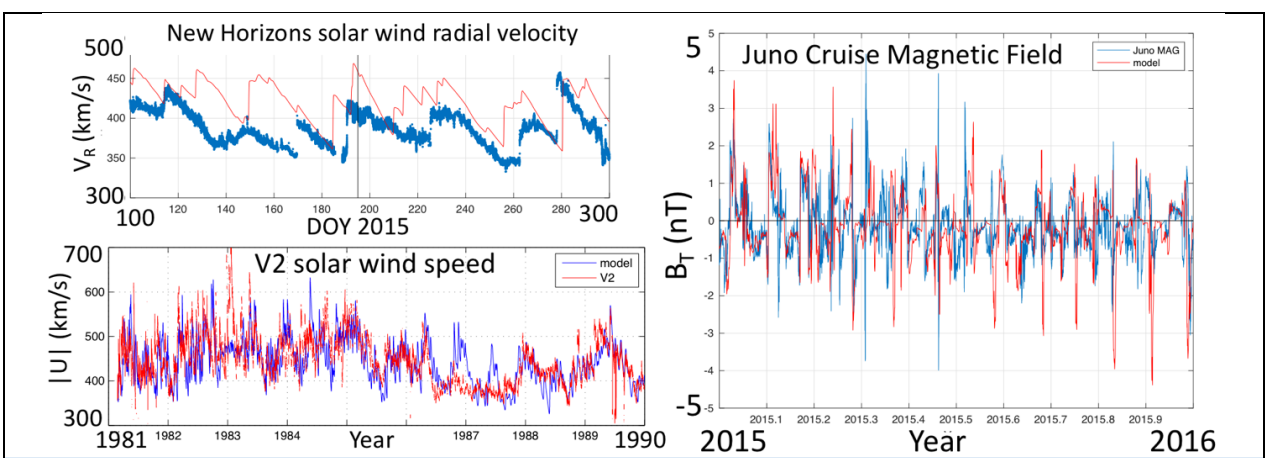

Figure 8. (top left) Predicted (red) and observed (blue) solar wind speed at New Horizons during the Pluto Flyby. **(bottom left)** Predicted (blue) and observed (red) solar wind speed at Voyager 2. **(right)** Predicted (red) and Juno MAG data (blue) during Juno's approach of Jupiter in 2015.

temperature. Model outputs include the solar wind density, plasma temperature, velocity, and all three components of the IMF at 1 hour resolution.

Collaborator Zieger has used SWMF-OH to predict the conditions at Pluto and along the New Horizons trajectory. It was one of the most successful models in the New Horizons Flyby Modeling Challenge at the Community Coordinated Modeling Center (CCMC). **Figure 8** (top left) demonstrates the reasonable fit between the predicted (red) and observed (blue) solar wind speed near Pluto. The model has been successfully validated with Pioneer 10 and Voyager 2 data (**Figure 8**, bottom left). **Preliminary results of solar wind propagation to Juno during its cruise phase to Jupiter (Moore et al., 2017), shown in Figure 8, demonstrate that not only the plasma parameters but also the interplanetary magnetic field (IMF) can be reasonably well predicted with the SWMF-OH at Jupiter's orbit.** The expected timing errors have not yet been quantified, but we will do so using the Juno cruise data. We anticipate that they will be roughly similar to mSWiM (10-15 hours for high recurrence index, ~35 hours for a low recurrence index).

The SWMF-OH model will be run on the NASA Pleiades supercomputer at the NASA Advanced Supercomputing (NAS) facility at NASA Ames. The model takes about a week to provide one entire year of propagated solar wind data at an hourly time resolution. If we encounter unexpected problems running SWMF-OH then we will run the mSWiM model, which was also created by Collaborator Zieger. mSWiM can be run on a desktop computer in a few days.

PI Vogt and Collaborator Zieger have funding from the NASA New Frontiers Data Analysis Program to run the SWMF-OH model from July 2016 through the end of 2018. That funding was awarded in early 2020 but the solar wind propagation work has not yet begun due to other projects and, in part, childcare issues associated with the COVID-19 pandemic. We expect to begin that work soon, and in doing so will work out any challenges with running the model so that the model runs we are proposing here should go smoothly. Finally, we note that the OMNI solar wind data model inputs (solar wind density, velocity, magnetic field, and temperature) have not yet been measured but this should not be considered to be a risk to our proposed work since our required model inputs are common data products that should be available for future space weather monitoring at Earth.

Expected results and their significance: We will produce new SWMF-OH predictions of the solar wind density, plasma temperature, velocity, and all three components of the IMF upstream of Jupiter during the Juno EM. As noted above, we plan to use the SWMF-OH outputs in our work for Tasks A, B, and C. **The predicted solar wind conditions upstream of Jupiter will be useful beyond just the work described in this proposal because it will provide context about the state of the magnetosphere, which will be useful to other Juno team members as they analyze Juno *in situ* data and auroral images from UVS.**

4. Research Team and Work Plan

PI Marissa Vogt will run the SWMF-OH solar wind propagation model in Task D, will perform the analysis of temporal variability that is part of Tasks A and B, and will perform Task C. PI Vogt will be responsible for the management of this investigation, including advising the graduate student, will also be responsible for compliance with all reporting requirements and implementation of the data management plan. PI Vogt is an expert on the structure and dynamics of Jupiter's magnetosphere and has worked extensively with Galileo and Juno magnetometer data at Jupiter (e.g. Vogt et al., 2010, 2014a, 2017, 2019, 2020). She has also worked with other Juno

and Galileo datasets and has studied Jupiter's magnetosphere through theoretical and numerical modeling (Vogt et al., 2011, 2014b, 2015).

A Boston University Graduate Student will perform the data analysis and work described in Tasks A and B. The FTE requested for the graduate student (6 months) exceeds the amount of effort requested for PI Vogt (3 months) because of PI Vogt's increased level of productivity, but PI Vogt will execute the majority of the work, including advising the graduate student. The graduate student's tasks are focused on Juno data analysis, rather than the solar wind model propagation, to enhance their participation in Juno science team activities.

Collaborator Bertalan Zieger will advise PI Vogt on running the SWMF-OH model to predict the solar wind conditions upstream of Jupiter (Task D). Collaborator Zieger is an expert in MHD modeling and developed the widely used mSWiM 1-D MHD solar wind propagation model (Zieger and Hansen, 2008; Zieger et al., 2009).

Our work plan is summarized in the following table. In all Years PI Vogt will advise the graduate student and manage the overall progress of the work in this proposal (0.5 months per year) and will attend Juno Science Team meetings (16 work days ≅ 0.75 months per year).

Year	Description
1 (Oct. 2022 - Sept. 2023)	**PI Vogt:** Run the SWMF-OH model for the start of the EM (June 2021) through the start of the project (Oct. 2022), then going forward on an orbit-by-orbit basis (Task D, 1 month). Characterize magnetic field temporal variability for Tasks A and B and compare to the predicted solar wind variability (0.5 months). Begin initial data-model comparison for Task C with available data from ~16:00-20:00 (0.25 months). **Graduate student:** For Task A, develop and test lobe field identification algorithm using available Juno dusk data and other datasets (2 months). Begin Task B analysis on available Juno dusk orbits (4 months).
2 (Oct. 2023 - Sept. 2024)	**PI Vogt:** Continue running the SWMF-OH model on an orbit-by-orbit basis (Task D, 0.5 months) and comparing predicted solar wind and magnetospheric variability (Tasks A and B, 0.5 months). Complete initial data-model comparison for Task C with available data from ~16:00-20:00 (0.25 months). **Graduate student:** Continue lobe identification and develop 2-D fits in Task A (1 month). Continue Task B analysis, prepare results for publication (5 months).
3 (Oct. 2024 - Sept. 2025)	**PI Vogt:** Continue running the SWMF-OH model on an orbit-by-orbit basis (Task D, 0.5 months). Complete the Task C data-model comparison with full local time coverage and prepare results for publication (1.25 months). **Graduate student:** Complete Task A, prepare results for publication (6 months).

We will post the solar wind propagation model results online for access by the Juno team and other members of the community as soon as possible. We have requested a period of performance of Oct. 22-Sept. 2025 to ensure solar wind predictions can be made for the full Juno EM. For each of Tasks A, B, and C we will publish a paper summarizing our results in a peer-reviewed journal.

5. Expected contributions to scientific return of the Juno mission and Relevance

Our proposed work enhances the scientific return of the Juno mission because our goals are distinct from, but complementary, to the Juno EM science objectives. Our work will characterize magnetospheric local time asymmetries and the general structure and dynamics of the duskside magnetosphere. Our work will therefore broaden the scientific return of the Juno mission because our work is distinct from the Juno EM science objective "Magnetosphere studies: Explore

the polar magnetopause and probe the polar cap auroral acceleration" listed in the Juno PSP call. However, our work will also contribute to the Juno EM science objectives. Task D will provide the modeled solar wind conditions upstream of Jupiter during the Juno EM, which will provide important context for the Juno data and analysis that addresses EM science goals "M2. Explore the region near Jupiter's polar magnetopause to investigate the interconnection and accessibility to the interplanetary medium" and "S1. Investigate satellite interactions with the Jovian magnetosphere and characterize Ganymede's magnetosphere". Specifically, the upstream solar wind conditions will help determine whether the magnetopause is in a likely compressed or expanded state (Joy et al., 2002). Additionally, the solar wind may influence the magnetic field in Jupiter's magnetosphere as close as Ganymede's orbit (Vogt et al., 2019) so the upstream solar wind conditions will provide context for analysis of the Galilean satellite flybys, which is important because magnetospheric conditions can influence the local satellite environment (e.g. Kivelson et al., 2004).

Our work further broadens the scientific return of the Juno mission because our work is focused on the middle and outer magnetosphere. However, previous and ongoing Juno team activities have been primarily focused on Juno's polar and inner magnetosphere (see for example the publication list maintained at http://lasp.colorado.edu/home/mop/bibliographies/juno-science-papers/). The inclusion of a graduate student in our proposal team will enhance participation in the Juno science team. PI Vogt is an expert on the structure and dynamics of Jupiter's magnetosphere (Vogt et al., 2010, 2011, 2014a, 2014b, 2015, 2017, 2019, 2020) who was selected as a Juno Participating Scientist in 2019. The work proposed here would ensure her continued ability to contribute to Juno science team activities, including working toward the EM science objectives.

In summary, this work is relevant to NASA and the Juno Participating Scientist program because it will use new Juno data to study the structure of Jupiter's magnetosphere. Our work will broaden and complement the science objectives of the Juno EM. Additionally, we have demonstrated here that publicly available datasets available on the PDS, including data from the Galileo and Ulysses missions, are insufficient for our proposed work because of their orbital coverage and data resolution, and that our work requires use of Juno EM data.

6. Relationship of the proposed work to current and pending funding

PI Vogt has received funding from the ROSES-2017 NASA Juno Participating Scientist program to identify tail reconnection events in Juno data and quantify the mass lost and flux closed by plasmoids, work which does not overlap with what we have proposed here. Furthermore, the period of performance of the ROSES-2017 Juno PS proposal and the work described here do not overlap, so there is no duplication of the requested travel funds for Juno science team meetings. (See http://sites.bu.edu/marissavogt/files/2019/07/vogt_juno_ps_2018_STM.pdf for Dr. Vogt's ROSES-2017 Juno PS proposal.) PI Vogt and Collaborator Zieger are funded by the New Frontiers Data Analysis Program to use SWMF-OH to predict the solar wind conditions upstream of Jupiter and draw comparisons to variability in Juno measurements from July 2016 through the end of 2018 but not for intervals during the Juno EM. Therefore, there is no overlap between our NFDAP-funded work (see https://sites.bu.edu/marissavogt/files/2019/11/vogt_nfdap19_public_stm.pdf) and the work proposed here.

References

Arridge, C., M. Kane, N. Sergis, K. K. Khurana, and C. M. Jackman. (2015). Sources of Local Time Asymmetries in Magnetodiscs. Space Science Reviews. 187. 301-333. 10.1007/s11214-015-0145-z.

Bagenal, F., R. J. Wilson, S. Siler, W. R. Paterson, and W. S. Kurth (2016), Survey of Galileo plasma observations in Jupiter's plasma sheet, J. Geophys. Res. Planets, 121, 871–894, doi:10.1002/ 2016JE005009.

Bonfond, B., Yao, Z., & Grodent, D. (2020). Six pieces of evidence against the corotation enforcement theory to explain the main aurora at Jupiter. Journal of Geophysical Research: Space Physics, 125, e2020JA028152. https:// doi.org/10.1029/2020JA028152

Clarke, J. T., J. Ajello, G. Ballester, L. B. Jaffel, J. Connerney, J.-C. Gérard, G. R. Gladstone, D. Grodent, W. Pryor, J. Trauger, and J. H. Waite Jr. (2002), Ultraviolet emissions from the magnetic footprints of Io, Ganymede and Europa on Jupiter, Nature, 415, 997.

Connerney, J. E. P., M. H. Acuña, N. F. Ness, and T. Satoh, (1998), New models of Jupiter's magnetic field constrained by the Io flux tube footprint, J. Geophys. Res., 103, 11929-11939.

Connerney, J.E.P., Benn, M., Bjarno, J.B. et al. (2017), The Juno Magnetic Field Investigation, Space Sci Rev 213: 39. https://doi.org/10.1007/s11214-017-0334-z

Connerney, J. E. P., Timmins, S., Herceg, M., & Joergensen, J. L. (2020). A Jovian magnetodisc model for the Juno era. Journal of Geophysical Research: Space Physics, 125, e2020JA028138. https://doi.org/10.1029/2020JA028138

Cowley, S. W. H., and E. J. Bunce (2001), Origin of the main auroral oval in Jupiter's coupled magnetosphere-ionosphere system, Plan. Space Sci., 49, 1067-1088.

Cowley, S. W. H., E. J. Bunce, T. S. Stallard, and S. Miller (2003), Jupiter's polar ionospheric flows: Theoretical interpretation, Geophys. Res. Lett., 30(5), 1220, doi:10.1029/2002GL016030.

Delamere, P. A., and F. Bagenal (2010), Solar wind interaction with Jupiter's magnetosphere, J. Geophys. Res., 115, A10201, doi:10.1029/2010JA015347.

Dungey, J. W. (1961), Interplanetary magnetic field and the auroral zones, Phys. Rev. Lett., 6, 47-48.

Frank, L. A., K. L. Ackerson, J. A. Lee, M. R. English, and G. L. Pickett (1992), The plasma instrumentation for the Galileo mission, Sp. Sci. Rev., 60, 283-307.

Gladstone, G.R., Persyn, S.C., Eterno, J.S. et al. (2014), The Ultraviolet Spectrograph on NASA's Juno Mission, Space Sci. Rev., 213: 447. https://doi.org/10.1007/s11214-014-0040-z

Grodent, D., Bonfond, B., Yao, Z., Gérard, J.-C., Radioti, A., Dumont, M., et al. (2018). Jupiter's aurora observed with HST during Juno orbits 3 to 7. Journal of Geophysical Research: Space Physics, 123, 3299– 3319. https://doi.org/10.1002/2017JA025046

Hess, S. L. G., E. Echer, and P. Zarka (2012), Solar wind pressure effects on Jupiter decametric radio emissions independent of Io, Planetary and Space Science, 70, 1, 114.

Hill, T. W. (2001), The Jovian auroral oval, J. Geophys. Res., 106, 8101-8107.

Joy, S. P., M. G. Kivelson, R. J. Walker, K. K. Khurana, C. T. Russell, and T. Ogino (2002), Probabilistic models of the Jovian magnetopause and bow shock locations, J. Geophys. Res., 107, 1309, doi: 10.1029/2001JA009146.

Khurana, K. K. (1992). A generalized hinged-magnetodisc model of Jupiter's nightside current sheet. Journal of Geophysical Research, 97, 6269–6276. 10.1029/92JA00169
Khurana, K. K. (1997), Euler potential models of Jupiter's magnetospheric field, J. Geophys. Res., 102(A6), 11295-11306.

Khurana, K. K. (2001), Influence of solar wind of Jupiter's magnetosphere deduced from currents in the equatorial plane, J. Geophys. Res., 106, 25999.

Khurana, K. K. and H. K. Schwarzl (2005), Global structure of Jupiter's magnetospheric current sheet, J. Geophys. Res., 110, doi:10.1029/2004JA010757.

Khurana, K. K., M. G. Kivelson, V. M. Vasyliūnas, N. Krupp, J. Woch, A. Lagg, B. H. Mauk, and W. S. Kurth (2004), The configuration of Jupiter's magnetosphere, in Jupiter: the Planet, Satellites, and Magnetosphere, edited by F. Bagenal et al., Cambridge Univ. Press, New York.

Kivelson, M. G., and K. K. Khurana (2002), Properties of the magnetic field in the Jovian magnetotail, J. Geophys. Res., 107(A8), 1196.

Kivelson, M. G. and D. J. Southwood (2005), Dynamical consequences of two modes of centrifugal instability in Jupiter's outer magnetosphere, J. Geophys. Res., 110, A12209, doi:10.1029/2005JA011176.

Kivelson, M. G., K. K. Khurana, J. D. Means, C. T. Russell, and R. C. Snare (1992), The Galileo magnetic field investigation, Space Sci. Rev., 60, 357-383.

Kivelson, M. G., Khurana, K. K., and Walker, R. J., Sheared magnetic field structure in Jupiter's dusk magnetosphere: Implications for return currents, J. Geophys. Res., 107(A7), doi:10.1029/2001JA000251, 2002.

Kivelson, M. G., F. Bagenal, W. S. Kurth, F. M. Neubauer, C. Paranicas, and J. Saur (2004), Magnetospheric Interactions with Satellites, in Jupiter: the Planet, Satellites, and Magnetosphere, edited by F. Bagenal et al., Cambridge Univ. Press, New York.

Kurth, W.S., et al. (2017), The Juno Waves Investigation, Space Science Reviews, 213, 347-392, doi:10.1007/s11214-017-0396-y.

Lorch, C. T. S., Ray, L. C., Arridge, C. S., Khurana, K. K., Martin, C. J., & Bader, A. (2020). Local time asymmetries in Jupiter's magnetodisc currents. Journal of Geophysical Research: Space Physics, 125, e2019JA027455. https://doi.org/ 10.1029/2019JA027455

Mauk, B.H., Haggerty, D.K., Jaskulek, S.E. et al. (2017), Space Sci Rev, 213: 289. https://doi.org/10.1007/s11214-013-0025-3

McComas, D.J., et al. (2017), The Jovian Auroral Distributions Experiment (JADE) on the Juno Mission to Jupiter, Space Science Reviews, 213, 547-643, doi:10.1007/s11214-013-9990-9.

Moore, L., J. O'Donoghue, H. Melin, T. Stallard, C. Tao, B. Zieger, J. Clarke, M. F. Vogt, T. Bhakyapaibul, M. Opher, G. Tóth, J. E. P. Connerney, S. Levin, and S. Bolton (2017), Variability of Jupiter's IR H3+ aurorae during Juno approach, Geophys. Res. Lett., 44, 4513–4522, doi:10.1002/2017GL073156.

Morgenthaler, J. P., Rathbun, J. A., Schmidt, C. A., Baumgardner, J., & Schneider, N. M., Large Volcanic Event on Io Inferred from Jovian Sodium Nebula Brightening, Astrophys. J., Lett., Vol. 871, No. 2, p. L23, 2019.

Northrop, T. G. and T. J. Birmingham (1982), Adiabatic Charged Particle Motion in Rapidly Rotating Magnetospheres, J. Geophys. Res., 87(A2), 661-669.

Opher, M. et al., Astrophys. J. Lett., 640, L71-L74, 2006.

Opher, M. et al., Nature, 462, 1036-1038, 2009.

Palmaerts, B., Vogt, M. F., Krupp, N., Grodent, D. and Bonfond, B. (2017), "Dawn-Dusk Asymmetries in Jupiter's Magnetosphere", in Dawn-Dusk Asymmetries in Planetary Plasma Environments (eds S. Haaland, A. Runov and C. Forsyth), John Wiley & Sons, Inc., Hoboken, NJ, USA. doi: 10.1002/9781119216346.ch24

Phipps et al. (2018), Distribution of Plasma in the Io Plasma Torus as Seen by Radio Occultation During Juno Perijove 1, J. Geophys. Res. Space Physics, 123, DOI:10.1029/2017JA025113

Phipps, P. H., Withers, P., Buccino, D. R., Yang, Y.-M., & Parisi, M. (2019). Variations in the density distribution of the Io plasma torus as seen by radio occultations on Juno Perijoves 3, 6, and 8. Journal of Geophysical Research: Space Physics, 124. https://doi.org/10.1029/2018JA026297

Ranquist, D. A., Bagenal, F., & Wilson, R. J. (2020). Polar flattening of Jupiter's magnetosphere. Geophysical Research Letters, 47, e2020GL089818. https://doi.org/10.1029/2020GL089818

Ray, L. C., N. A. Achilleos, M. F. Vogt, and J. N. Yates (2014), Local time variations in Jupiter's magnetosphere-ionosphere coupling system, J. Geophys. Res. Space Physics, 119, 4740-4751, doi:10.1002/2014JA019941.

Tao, C., R. Kataoka, H. Fukunishi, Y. Takahashi, and T. Yokoyama (2005), Magnetic field variations in the Jovian magnetotail induced by solar wind dynamic pressure enhancements, J. Geophys. Res., 110, A11208, doi:10.1029/2004JA010959.

Thomas, N., F. Bagenal, T. W. Hill, and J. K. Wilson (2004), in Jupiter: the Planet, Satellites, and Magnetosphere, edited by F. Bagenal et al., Cambridge Univ. Press, New York.

Tóth, G. et al., J. Comp. Phys., 231, 870-903, 2012.

Vasyliūnas, V. M. (1983), Plasma distribution and flow, in Physics of the Jovian Magnetosphere, edited by A. J. Dessler, p. 395, Cambridge Univ. Press, New York.

Vogt, M. F., M. G. Kivelson, K. K. Khurana, S. P. Joy, and R. J. Walker (2010), Reconnection and flows in the Jovian magnetotail as inferred from magnetometer observations, J. Geophys. Res., 115, A06219, doi: 10.1029/2009JA015098.

Vogt, M. F., M. G. Kivelson, K. K. Khurana, R. J. Walker, B. Bonfond, D. Grodent, and A. Radioti (2011), Improved mapping of Jupiter's auroral features to magnetospheric sources, J. Geophys. Res., 116, A03220, doi:10.1029/2010JA016148.

Vogt, M. F., C. M. Jackman, J. A. Slavin, E. J. Bunce, S. W. H. Cowley, M. G. Kivelson, and K. K. Khurana (2014a), Structure and Statistical Properties of Plasmoids in Jupiter's Magnetotail, J. Geophys. Res. Space Physics, 119, 821-843, doi:10.1002/2013JA019393.

Vogt, M. F., M. G. Kivelson, K. K. Khurana, R. J. Walker, M. Ashour-Abdalla, and E. J. Bunce (2014b), Simulating the Effect of Centrifugal Forces in Jupiter's Magnetosphere, J. Geophys. Res. Space Physics, 119, 1925-1950, doi:10.1002/2013JA019381.

Vogt, M. F., E. J. Bunce, M. G. Kivelson, K. K. Khurana, R. J. Walker, A. Radioti, B. Bonfond, and D. Grodent (2015), Magnetosphere-ionosphere mapping at Jupiter: Quantifying the effects of using different internal field models, J. Geophys. Res. Space Physics, doi:10.1002/2014JA020729.

Vogt, M. F., E. J. Bunce, J. D. Nichols, J. T. Clarke, and W. S. Kurth (2017), Long-term variability of Jupiter's magnetodisk and implications for the aurora, J. Geophys. Res., doi:10.1002/2017JA024066.

Vogt, M. F., S. Gyalay, E. A. Kronberg, E. J. Bunce, W. S. Kurth, B. Zieger, and C. Tao (2019), Solar wind interaction with Jupiter's magnetosphere: A statistical study of Galileo in situ data and modeled upstream solar wind conditions, J. Geophys. Res. Space Physics, doi:10.1029/2019JA026950.

Vogt, M. F., Connerney, J. E. P., DiBraccio, G. A., Wilson, R. J., Thomsen, M. F., Ebert, R. W., et al (2020). Magnetotail reconnection at Jupiter: A survey of Juno magnetic field observations. Journal of Geophysical Research: Space Physics, 125, e2019JA027486. https://doi.org/10.1029/2019JA027486

Williams, D. J., R. W. McEntire, S. Jaskulek, and B. Wilken (1992), The Galileo energetic particles detector, Space Sci. Rev., 60, 385-412.

Woch, J., N. Krupp, and A. Lagg (2002), Particle bursts in the Jovian magnetosphere: Evidence for a near-Jupiter neutral line, Geophys. Res. Lett., 29, 1138-1141, doi:10.1029/2001GL014080.

Zieger , B. and K. C. Hansen (2008), Statistical validation of a solar wind propagation model from 1 to 10 AU, J. Geophys. Res., 113, A08107, doi:10.1029/2008JA013046.

Zieger, B., Hansen, K. C., Cohen, O., Gombosi, T. I., Zurbuchen, T. H., Anderson, B. J., and Korth, H. (2009), Upstream conditions at Mercury during the first MESSENGER flyby: Results from two independent solar wind models, Geophys. Res. Lett., 36, L10108, doi:10.1029/2009GL038346.

Data Management Plan

1. Overview of the data that will be produced by the proposed project, including expected data types, volume, and formats.

In Task A we will develop an algorithm to identify times when the Juno spacecraft is in the tail lobes as indicated by plateaus in the magnetic field magnitude. We will derive lists of lobe field intervals that will be included in tables or as supplemental information in peer-reviewed publications (ASCII/plain text, small in volume – less than 1 MB).

In Task B we will calculate the 10-hour running average of the field bendback angle, which we will produce with a 1-minute time resolution. We will output a data file that contains the date, time, and bendback angle 10-hour running average that will be included as supplemental information in peer-reviewed publications (ASCII/plain text, estimated 100 MB volume for the field bendback angle measured over the entire Juno mission).

Task C, in which we will compare Juno JADE and JEDI data to output from a previously-published large-scale kinetic simulation, will produce no new data.

The outputs of Task D will be SWMF-OH model predictions of the solar wind conditions (velocity, density, etc.) upstream of Jupiter during the Juno extended mission (mid-2021 through 2025). These will be produced as plain ASCII files with the plasma and magnetic field parameters. We expect the file size to be no larger than 10 MB for each full year of predicted solar wind data.

2. Schedule for data archiving and sharing:

We will make the outputs of Task D, the predicted solar wind conditions upstream of Jupiter, available to the community via PI Vogt's Boston University website (http://sites.bu.edu/marissavogt/) as soon as the model outputs are finalized (i.e. we will not wait for the accompanying paper to be published, since we expect the model outputs will be immediately useful to Juno team members and others in the community). However, we will also archive the data with Zenodo to ensure its long-term preservation.

All other data will be included in tables or in supplemental material accompanying publications as stated above. We will also post data files to PI Vogt's BU website within one month of paper publication.

3. Intended repositories for archived data and mechanisms for public access and distribution, and plan for enabling long-term preservation of the data:

All data will be included in tables or in supplemental material accompanying publications, which we expect will be submitted to AGU journals like JGR or GRL. Zenodo and most reputable publishers have robust plans in place for long-term preservation of the data they curate.

4. Software archiving plan:

For data analysis tasks that involve developing a new technique or method, created specifically for the data used in our study, we will include our analysis technique or code as part of the supplemental online information published with each paper. An example of this type of

analysis software would be the algorithm that we will develop to identify lobe field intervals in Task A. We will also post our code to NASA GitHub and PI Vogt's BU website within one month of manuscript acceptance.

The solar wind model prediction runs in Task D use an existing model, SWMF-OH, so no software will be generated. However, we will explore the possibility of making the model available on the Community Coordinated Modeling Center (CCMC) website so that users can run the model upon request.

5. Roles and responsibilities of team members for data management:

PI Vogt will assume all responsibilities associated with this DMP, with assistance from the graduate student.